Changes in precipitation extremes for New Zealand: climate model predictions

Trevor Carey-Smith[1a)], Sam Dean[a)], Jessica Vial[b)], Craig Thompson[a)]

[a)]*National Institute of Water and Atmospheric Research, Wellington, New Zealand*

[b)]*Victoria University of Wellington, Wellington, New Zealand*

Abstract

An analysis of daily precipitation output from a regional climate model was undertaken in order to estimate future changes in precipitation extremes for New Zealand. Daily rainfall for present (1971—2000) and future (2071—2100) climate under the Intergovernmental Panel on Climate Change Special Report on Emissions Scenarios A2 and B2 emission scenarios, was simulated by the regional climate model PRECIS, developed at the UK Met Office Hadley Centre. Return values of 1-day precipitation extreme for a 5-year return period were calculated from a generalized Pareto extreme value model fitted to the tail of the rainfall distribution. A test of the statistical analysis in several regions of New Zealand revealed that the generalized Pareto model was appropriate for estimating daily precipitation extremes over the country for short return periods, but was unable to realistically capture the changes in longer return periods under transient climate change. For long return periods, a separate analysis of the regional climate model simulations suggested that the increase in the heaviest rainfall extremes in the country has an upper limit in the range of between 7 to 9% per Kelvin of warming. Similarly, an ensemble of global climate models from the Coupled Model Intercomparison Project 3, suggested an increase of 5 to 12% per Kelvin. For New Zealand, increases in precipitation extremes greater than that predicted by the widely used Clausius Clapeyron relationship (6.5% per Kelvin), should be considered in future planning.

---

1 Corresponding author address: Trevor Carey-Smith, NIWA, Private Bag 14 901, Kilbirnie, Wellington, New Zealand. E-mail: t.careysmith@niwa.co.nz

1. Introduction

Extreme rainfall is defined as a “rare” event generating a relatively high amount of precipitation. The characteristics of precipitation extremes vary spatially according to the physical nature of a region (such as the presence of mountains or large bodies of water), however, the less frequent a high rainfall event occurs in a region, the more extreme it is classified. Heavy rainfall events can produce flooding, which often causes damage to infrastructure and can have a serious impact on the agricultural industry.

Many studies using different methods have been undertaken to estimate changes in the frequency and the intensity of extreme precipitation events. One such study in the New Zealand context (Griffiths, 2007) analysed historical trends in rainfall extremes using indices of extremity from daily station data for the periods 1930-2004 and 1950-2004, and found that high rainfall events are highly correlated with circulation. Griffiths (2007) defined two indices of rainfall extremity named “the very wet day” and ”the extremely wet day”, calculated as the 95th and 99th percentile rainfall value respectively. Temporal trends in the indices showed a west-east pattern across the mountains of both islands for both periods, with an increase of extreme precipitation in the west, and a decrease in the east. A seasonal analysis over the period 1958-2004 exhibited decreased summer extreme precipitation in eastern areas of both islands, and increased extremes in winter and spring in the western South Island.

Regional climate models have become important tools for evaluating how local rainfall extremes might change in the future. In a leading example of this approach, Frei *et al.* (2006) analysed changes in precipitation extremes in Europe using extreme value theory, based on six European regional climate models for present (1971-1990) and future (2071-2100) climate under the Intergovernmental Panel on Climate Change (IPCC) Special Report on Emissions Scenarios (SRES) A2 emission scenario (Nakicenovic *et al.* 2000). Quantiles of 1 and 5-day precipitation extreme for return periods of 2, 5, 10, 20, 50 and 100 years were estimated from a generalized extreme value distribution fitted to seasonal precipitation maxima. The results indicated good agreement between the models for

an increase in the frequency of precipitation extremes in northern parts of Europe and a decrease in the south.

The purpose of the study presented in this paper was to examine possible methods of using climate model output in order to estimate changes in precipitation extremes for New Zealand resulting from climate change. This was initially done by analysing output from a regional climate model using the statistical method of extreme value theory. Subsequently, comparisons were made between the regional climate model and global climate models from the World Climate Research Programme's (WCRP's) Coupled Model Intercomparison Project phase 3 (CMIP3, Meehl *et al.* 2007). This was done in an attempt to elucidate the maximum possible change for the country's heaviest rainfall extremes, and to also encompass some of the uncertainty associated with using different climate models.

2. Data Sets and Methods

a. Data Sets

1) OBSERVATIONS

This analysis used an observational rainfall data set created on a 0.27° latitude/longitude grid covering all of New Zealand for a 29-year period (1972—2000). The daily rainfall surface was estimated using a second-order derivative trivariate thin plate smoothing spline spatial interpolation model, incorporating the longitude and the latitude as location variables, and a mean annual rainfall variable (Tait *et al.*, 2006). The process minimises the generalized cross validation by fitting a smooth surface to the data which incorporates a small error at each data point. The interpolation is performed with an *a-priori* square root transformation of the daily rainfall observations (and subsequent back transformation) on a complete subset of 128 climate station daily rainfall records. The square root transformation is used to help in normalizing positively skewed data sets, reducing the standard errors in the fitted surfaces. The weakness of this method is that it can result in poor interpolation in areas with a low density network of climate stations, possibly missing very localized rainfall events. Furthermore, it has been shown by Tait *et al.* (2006) that

interpolation often underestimates rainfall in some areas, especially at relatively high altitudes. For this study, the rainfall surface from Tait *et al.* (2006) was interpolated to the resolution of the regional climate model (~30 km) using a bilinear interpolation and is referred to as VClim for the remainder of this paper. The deficiencies mentioned above meant that VClim was not an ideal benchmark for this study on extreme precipitation, particularly in regions of low station density, however the data set allowed for spatial comparisons which were not possible with raw station observations.

In addition to the VClim gridded data set, a selection of observing stations were used to investigate the effect interpolation has on extreme rainfall events (Figure 1). These stations were selected to be representative of the different rainfall regimes around the country and all have data available for the full 29 years.

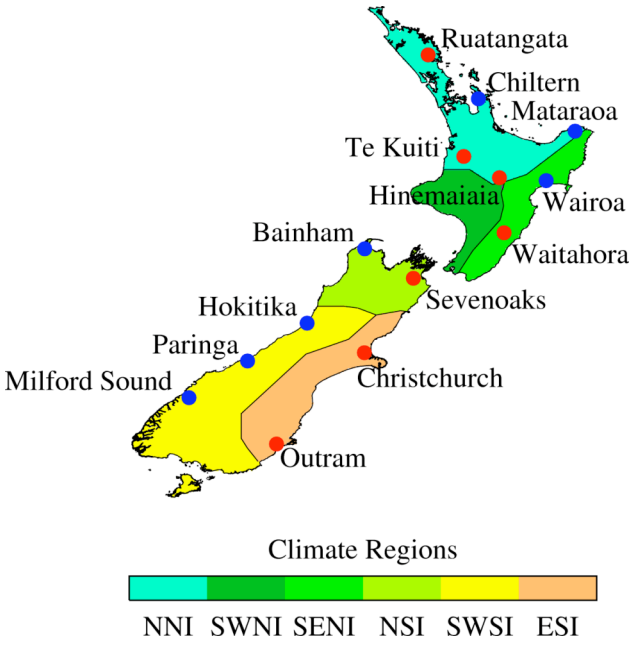

Figure 1: Locations of climate stations and regions used in this study. Stations with relatively high (low) rainfall are shown with blue (red) dots. Coloured shading demarcates six coherent climate regions identified by Mullan (1998) who used a rotated EOF analysis of rainfall data to isolate parts of New Zealand within which the characteristics of the mean rainfall are relatively similar.

2) SIMULATIONS

This study used data sets of 24-hour rainfall totals simulated by the PRECIS regional climate model (RCM, HadRM3P, Jones *et al.*, 2004) and its parent global climate model (GCM, HadAM3P, Jones *et al.*, 2005), both developed at the UK Met Office Hadley Centre. Use was also made of 16 global climate models from the CMIP3 multi-model data set. These models were all run under the IPCC SRES A2 emission scenario.

The RCM was run twice for a 30-year time slice of present climate (1971—2000); once from boundary conditions produced by the global model with observed sea surface temperatures (Control), and once by boundary conditions taken from ERA-40 reanalyses (Reanalyses). Observed sea surface temperatures (HadISST2) were used in both cases. An ensemble of three future climate simulations (2071—2100) was also generated; two under the A2 emission scenario (A2 Run 1; A2 Run 2) and one under the B2 emission scenario (B2 Run 1). The A2 scenario consists of "relatively high" emissions from a world focussed on nation states and with continuously increasing population. The B2 emission scenario has lower emissions than the A2 scenario, with much slower population growth and an emphasis on local solutions to environmental and social issues (Rowell, 2005).

It should be noted that the maximum altitude of the Southern Alps was not fully resolved by the 30 km resolution RCM. The highest gridbox in the RCM was at 2400 m while in reality numerous peaks exceed 3000 m. This model resolution meant that it is likely some orographically induced localised rainfall events were not simulated by the RCM. However, it was the change in extreme precipitation that was of primary interest in this study and this does not explicity depend on having the full range of precipitation event magnitudes simulated.

b. Methods

This study used extreme value theory (EVT) to estimate future changes in precipitation extremes within New Zealand. EVT is well developed, and has been used by several groups for analysing extreme hydrological events (Frei *et al.*, 2006; Li *et al.*, 2005; Madsen *et al.*, 1997; Rosbjerg *et al.*, 1992), as well as extreme wind

speeds (Brabson and Palutikof, 2000; Pandey *et al.*, 2001). Frei *et al.* (2006) used the annual precipitation maxima to estimate return values of extreme rainfall, which meant that other significant events available in the data were omitted. An alternative method is the peaks over threshold (POT) analysis (also called partial duration series) which uses rainfall events that exceed a carefully selected high threshold (Coles, 2001). In this study, the POT method was used to select extreme events to which a Generalized Pareto Distribution (GPD) was then fitted (May, 2007; Yiou *et al.*, 2008). The methodology is now outlined in detail.

1) THE PEAKS OVER THRESHOLD APPROACH

Let the random variable X denote the daily rainfall observation with an unknown distribution G. The peaks over threshold (POT) approach consists of estimating the conditional probability that X is less than x given that X exceeds some threshold x_0, such that

$$\Pr(X \le x \mid X > x_0) = \frac{1-\mathrm{G}(x)}{1-\mathrm{G}(x_0)}, \text{ for } x > x_0. \tag{1}$$

Pickands (1975) showed that as the threshold x_0 becomes large, the conditional distribution converges to a GPD with a shape k and a scale a as parameters. The GPD has a distribution function

$$\mathrm{F}(x) = \begin{cases} 1-\left(1-\dfrac{k\left(x-x_0\right)}{a}\right)^{\frac{1}{k}}, \text{ for } k \neq 0 \\ 1-\exp\left(-\dfrac{x-x_0}{a}\right), \text{ for } k = 0. \end{cases} \tag{2}$$

When $k > 0$, the distribution has zero probability density for $x \ge \left(a/k\right) + x_0$, while for $k < 0$, there is no upper bound ($x_0 \le x \le \infty$). The special case $k = 0$, yields the exponential distribution with mean a (Hosking and Wallis, 1987).

The POT approach involves the choice of an appropriate threshold level, x_0, which, in this study, was calculated from the mean, $\mathrm{E}(X)$, and standard deviation, $\mathrm{S}(X)$, of the daily rainfall distribution as

$$x_0 = \mathrm{E}(X) + q\,\mathrm{S}(X) \quad (3)$$

where $q \geq 0$ (Madsen *et al.*, 1994). This approach is advantageous as it uses the characteristics of the distribution in question to calculate the threshold rather than some arbitrary fixed definition of threshold (such as 50 mm within 6 hours).

An important property of a Generalised Pareto Distribution, X, is that $X - x_0$ is also a GPD with the same shape parameter k, given that $X > x_0$ (Rosbjerg *et al.*, 1992). This means that for sufficiently high threshold, k is nearly constant. Figure 2 shows how k varied depending on the threshold parameter, q, for two representative sites. Data from actual climate stations are shown along with the nearest gridpoint from the gridded observational data set and the control and reanalyses RCM runs. For q between 1 and 2, the shape parameter was reasonably flat for all data sources. Below q 1, k often had a positive slope and above q 3, k began to diverge. Using a value of $q = 2$, provided threshold values between 7 and 14 mm for Outram and between 45 and 65 mm for Bainham. Using these threshold values meant that the number of exceedances stayed constant at approximately 500 (out of a total of ~10500 days) for all data sources from both of these sites. A similar analysis for a number of different representative climate stations across New Zealand confirmed $q = 2$ as a suitable choice for application of POT to New Zealand rainfall.

2) EVENT INDEPENDENCE

An important assumption of the statistical theory of extreme value analysis states that consecutive exceedances have to be independent, which is often violated when using real geophysical observations. Indeed, hydrological events often last several days, so a daily rainfall event may often be related to one on an adjacent day. However, according to previous work done in this area the temporal dependence in daily rainfall series is weak at the level of extremes (Coles, 1994).

The partial duration series method involves the selection of an appropriate threshold level, which should be large enough to make this assumption valid. In this study two approaches were used to check whether it was reasonable to assume that

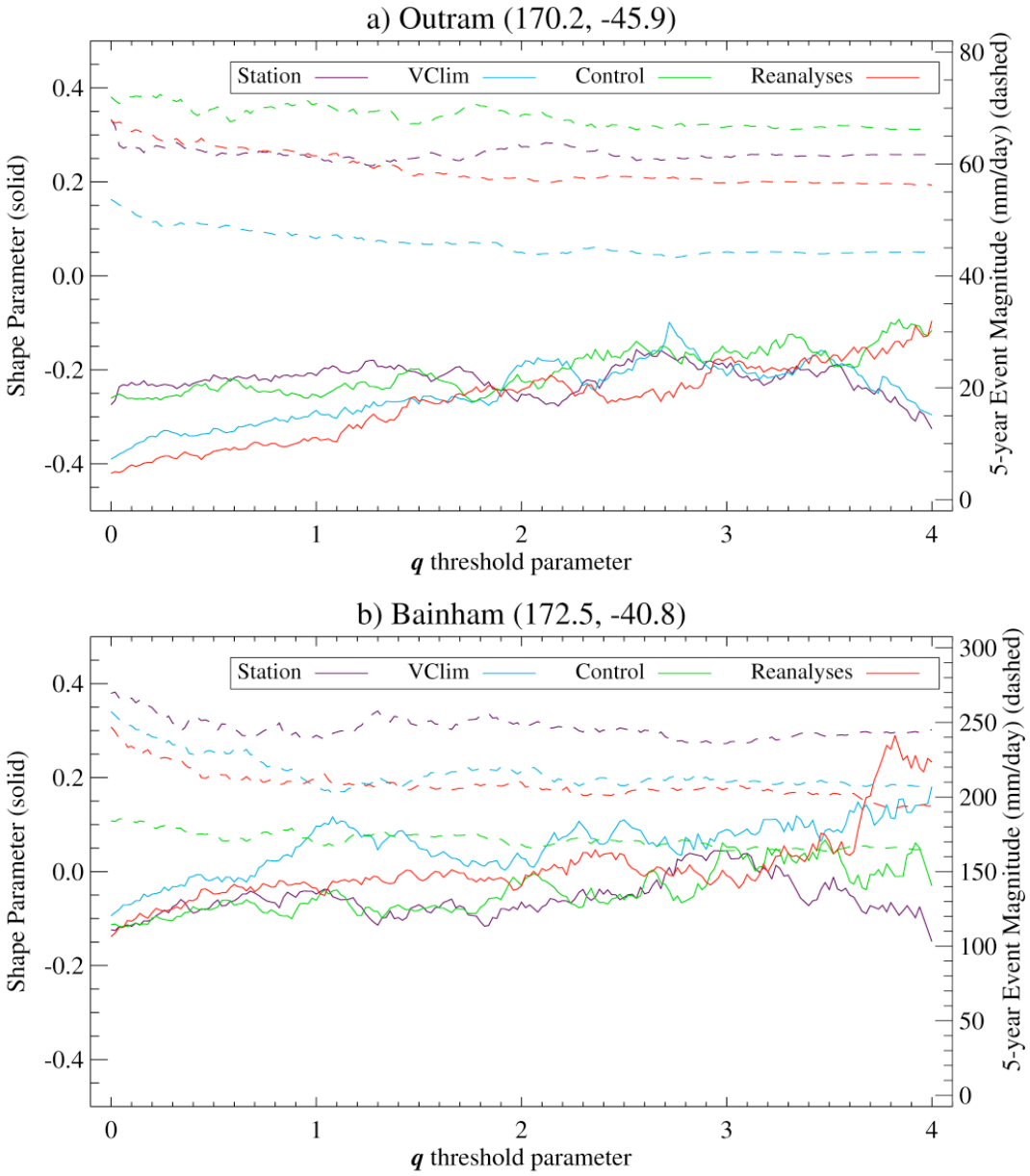

Figure 2: Relationship of the q threshold parameter to both the shape parameter k (solid) and T-year event magnitude (dashed). Outram (a) is a relatively dry location on the east coast of the South Island and Bainham (b) is a wet location on the northern tip of the South Island. Site longitude and latitude are shown in brackets.

the exceedances were independent. By comparing the magnitudes of successive rainfall exceedances, it was possible to identify the level of dependence between the magnitude of extreme events. This was done for a selection of sites and it was found that the correlation between successive exceedances was very close to zero (R typically less than 0.07).

The second approach used was based on physical considerations, and consisted of analyzing the number of days between consecutive extreme events. If events were not independent, it was expected that successive events more closely spaced in time would be more highly correlated than those with larger separation. Analysis of a selection of observing sites with rainfall records longer than 100 years showed that about 15% of exceedance events occurred on consecutive days. The correlation between successive events grouped by separation is shown in Figure 3. With the exception of Stephens Island, a decrease in correlation with increased separation time was not observed, suggesting that the assumption of event independence was not unreasonable. The increased spread in R with increasing separation time was due to the decreasing sample size.

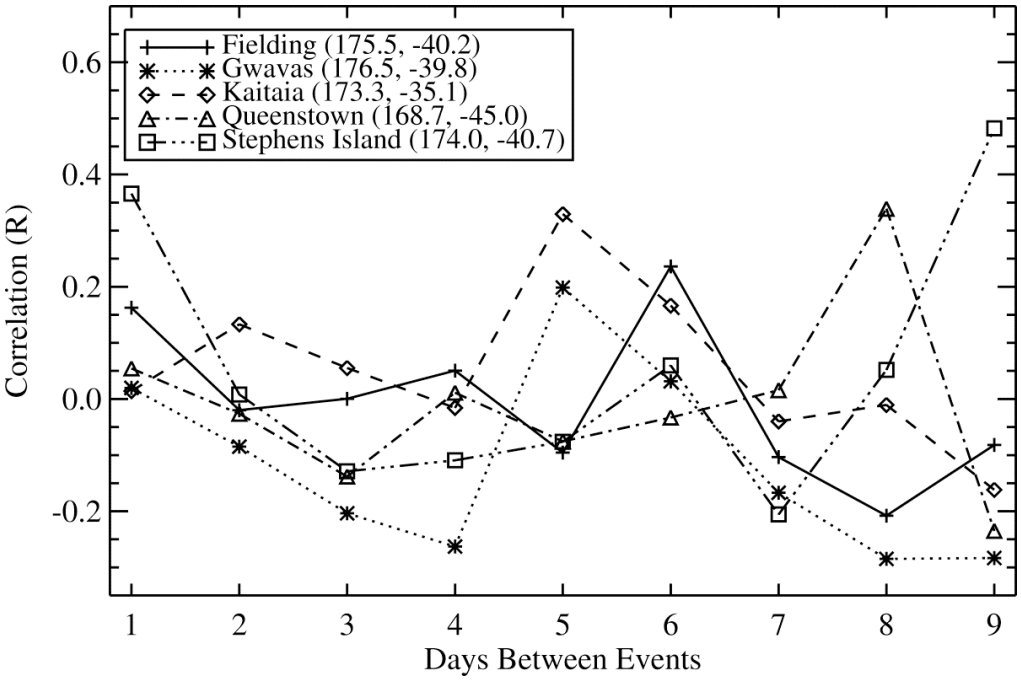

Figure 3: Correlation between successive rainfall exceedances. The five climate stations shown (longitude and latitude shown in brackets) each have rainfall records longer than 100 years.

3) PARAMETER ESTIMATION

Once a suitable threshold has been determined, the parameters of the GPD can be estimated by the *L*-moments method, also referred to as linear combinations of expectations of order statistics (Hosking, 1990). This method is very powerful in parameter estimation as compared to other methods, such as maximum likelihood or the method of moments. It has the advantage of being less influenced by outliers and less subject to bias estimation. This method is particularly useful for small samples since the *L*-moments remain fairly accurate.

The shape factor k and scale factor a of the GPD can then be found using estimates of the first and second *L*-moments, λ_1 (sample mean) and λ_2,

$$\begin{aligned} k &= \frac{1}{\tau_2} - 2 \\ a &= \lambda_1 \left(\frac{1}{\tau_2} - 1 \right) \end{aligned} \tag{4}$$

where $\tau_2 = \lambda_2 / \lambda_1$ is an estimate of the *L* coefficient of variation (Hosking, 1990).

4) ESTIMATION OF THE *T*-YEAR EVENT

If the GPD with parameters a and k is a suitable model for rainfall exceedances above a threshold x_0, then the return level x_m can be defined as the precipitation intensity that is exceeded on average once every m observations. Therefore using equation (2), for $x_m > x_0$,

$$\frac{1}{m} = 1 - \Pr\left(X \le x_m\right) = \begin{cases} \left(1 - \dfrac{k\left(x_m - x_0\right)}{a}\right)^{\frac{1}{k}}, \text{ for } k \neq 0 \\ \exp\left(-\dfrac{x_m - x_0}{a}\right), \text{ for } k = 0. \end{cases} \tag{5}$$

It is convenient to interpret return levels on an annual time scale, so that the *T*-year return level is the level expected to be exceeded on average once every *T* years. So if there are λ observations per year, this corresponds to the m-

observation return level, where $m = \lambda T$. Therefore, from equation (5) the *T*-year event, x_T as defined by (Madsen *et al.*, 1997) is

$$x_T = \begin{cases} x_0 + \frac{a}{k}\left(1 - \left(\frac{1}{\lambda T}\right)^k\right), \text{ for } k \neq 0 \\ x_0 + a \ln\left(\lambda T\right), \text{ for } k = 0. \end{cases} \quad (6)$$

Figure 2 shows how the 5-year event magnitude varied with threshold for two representative sites. The event magnitude was relatively flat for $q > 1$ giving further confidence in the value $q = 2$ chosen for this study.

3. Results

a. Regional Climate Model Evaluation

In this section, an evaluation of the mean daily rainfall and precipitation extremes for the present climate (1972—2000) as simulated by the regional climate model (RCM) is presented. The results from the 20th century RCM simulations were compared with the gridded observational data set VClim as well as individual stations.

Figure 4 shows some examples of the Generalised Pareto Distribution applied to extreme rainfall data, plotted against a logarithmic percentile axis to highlight the structure of the extremities. When daily rainfall data are displayed in this way, the 99.9 percentile is roughly equivalent to an average return interval of 3 years and the 99.99 percentile to a 1 in 30 year event.

For Milford Sound, the observations and RCM simulations all showed a smooth increase until between the 99.9 and 99.95 percentile, at which point a dip in the tail was observed (solid lines). The modelled GPD curves for $q = 2$, while generally a good fit up to the 99.95 percentile, failed to fit this dip (dashed lines). The difference between the GPD fits to the control and the A2 run1 continued to grow indefinitely as the percentile was increased. In fact the actual data suggested that the difference between the two runs became constant.

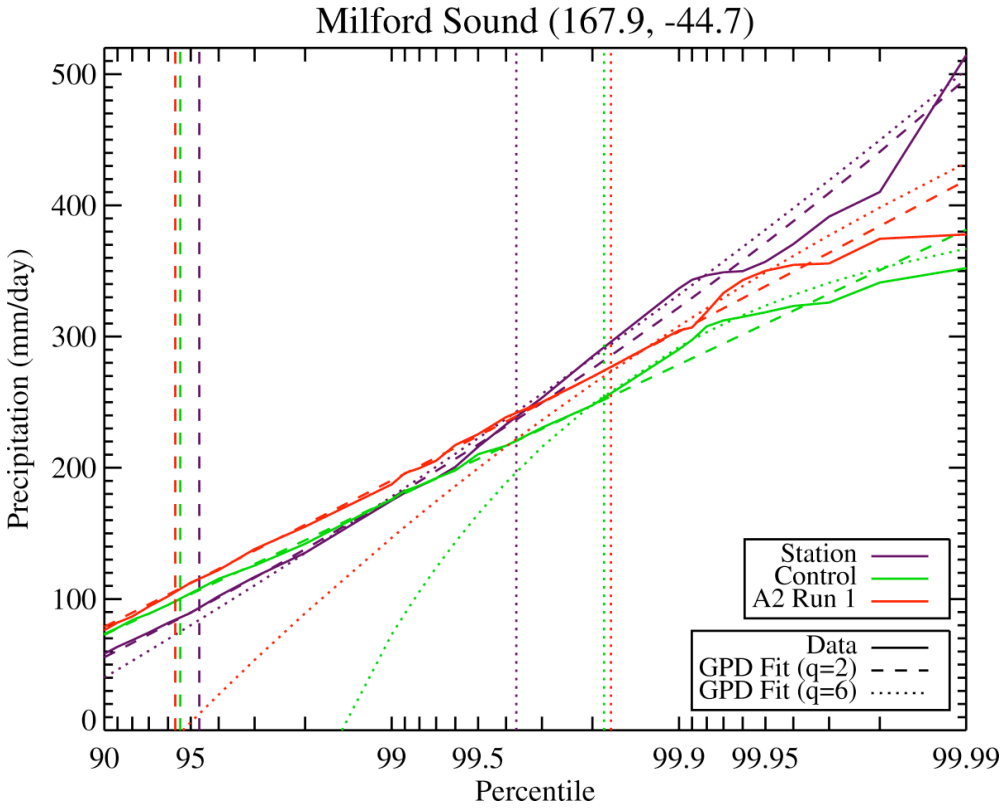

Figure 4: Logarithmic percentile plot of daily precipitation for Milford Sound. Data from the climate station (purple), the RCM Control (green) and the RCM A2 Run 1 simulation (red) are shown by the solid lines. Two different GPD fits to each of these data sets are also shown. The vertical lines correspond to the threshold used in the computation of each GPD. For these 30 year time series, the 99.99 percentile contains a single point, hence it is inherently noisy.

An approach taken by some researchers has been to limit the shape parameter to be positive, and determine the threshold from the subsequent goodness of fit. In Figure 4 the GPD fit for a high threshold of $q = 6$ is also displayed. Even with this threshold the best fit was not always a positive shape parameter, and negative fits were not necessarily any better then the original fits. In fact, it was found that in most cases the shape parameter became highly unstable at these high thresholds, which contravenes the assumptions underlying the use of the GPD. Here it is suggested that a three parameter polynomial is required to adequately fit both modelled and observational data in a POT analysis. This was not attempted in the study but remains an area for further investigation. In summary, our analysis suggested that the method described here was only able to accurately characterise

changes up to return periods of 3—5 years, and as such results are not presented beyond this time-frame. This short return period still allows for consideration of the regional changes observed in the model under a future climate.

1) DAILY MEAN RAINFALL

The mean daily rainfall distribution over New Zealand for the RCM (Control) and the observational data set (VClim), as well as their percentage difference, are shown in the upper plots in Figure 5. The RCM reproduced the observed daily mean precipitation pattern quite well; exhibiting the strong west-to-east mean rainfall gradient in the South Island, due to the dominant westerly winds interacting with the main mountain range.

The percentage difference, shown in the upper right plot, indicated that much of the country was drier in the RCM, especially in the regions of Canterbury, Hawkes Bay/Gisborne, New Plymouth, as well as in Northland and in southern South Island where the mean rainfall was underestimated by more than 50%. On the other hand the mountainous areas experienced wetter conditions, and the largest differences seemed to occur on the top of the mountain ranges in the South Island where the RCM overestimated observations by up to 100%. This positive error may not be entirely model error as the gridded data set is known to underestimate rainfall amounts in high mountain regions (Tait *et al.*, 2006).

2) PRECIPITATION EXTREMES

The 5-year return interval 1-day extreme precipitation amounts generated by the observational data set and the RCM control are displayed in the lower plots in Figure 5. The largest return values from both the RCM and the observations were along the west coast in the South Island, with relatively high return values also observed along the east coast of the North Island. This is to be expected as heavy precipitating systems in New Zealand are often associated with advection and convergence of moist air masses of subtropic and/or polar origin. Rainfall extremes mostly occur by orographic lifting, but they can also arise from convective showers embedded in weather systems.

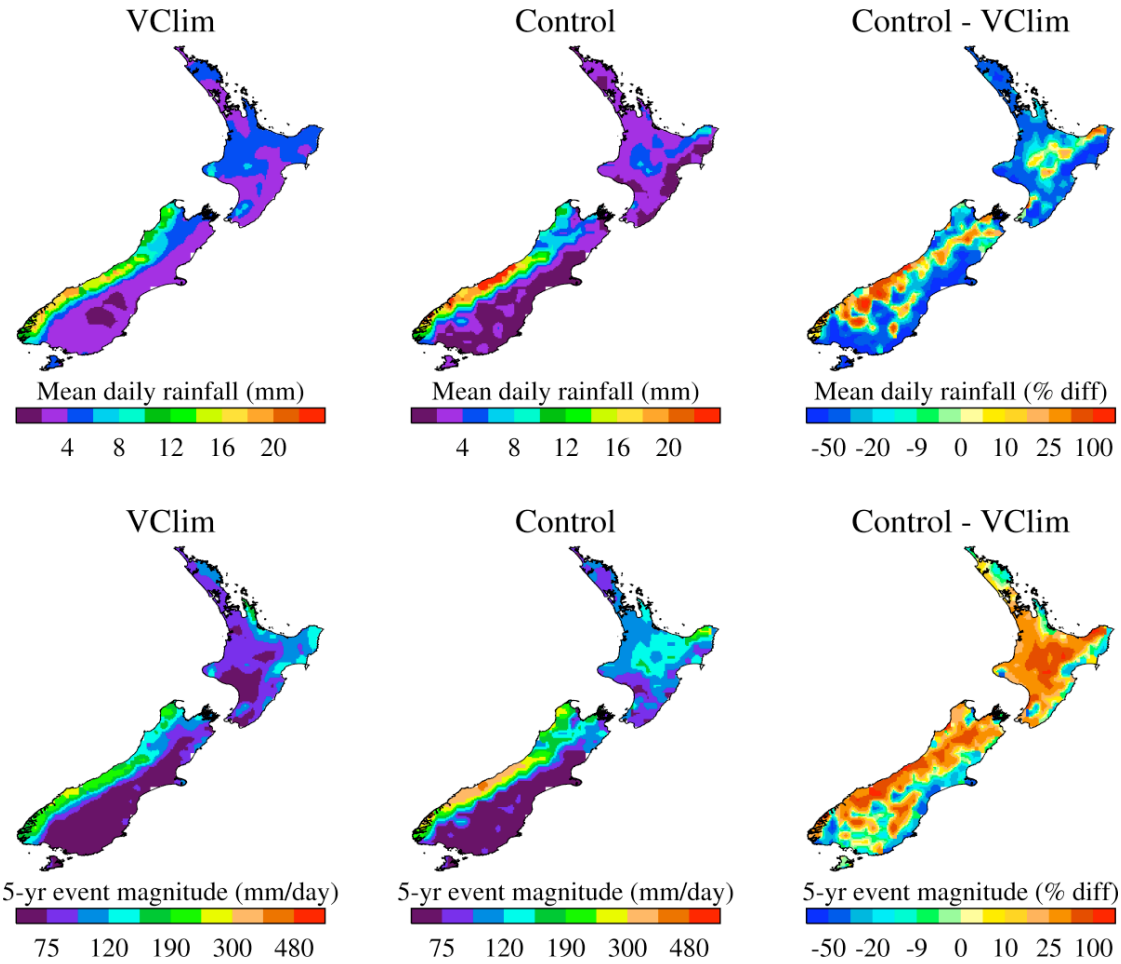

Figure 5: Comparison between the gridded observations and the RCM control run for mean daily rainfall (top row) and the 5-year event magnitude (bottom row).

There were, however, significant differences between the gridded observations and RCM control run. The percentage differences (lower right plot of Figure 5) suggest that the RCM tended to overestimate extreme rainfall events especially in the mountain ranges of both islands. Although a similar pattern was observed in the mean of the daily rainfall distribution, it was much more pronounced in the extreme rainfall distribution. Either the RCM overestimated extreme rainfall events, or the interpolation of the observational data set introduced too much smoothing.

3) ERA-40 REANALYSES

An RCM simulation driven by boundary conditions taken from ERA-40 reanalyses was performed to quantify the effect any biases in the GCM circulation may have had on the mean and extreme rainfall (Figure 6).

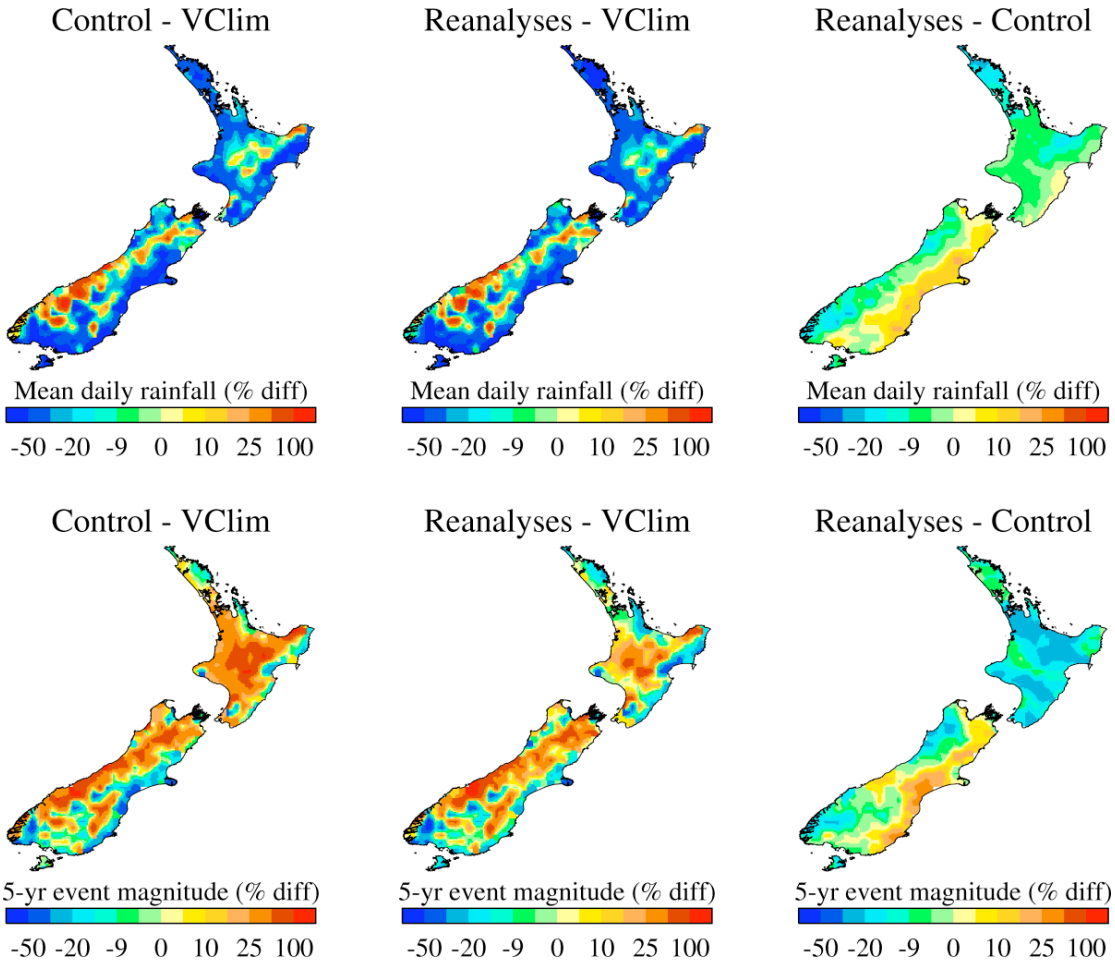

Figure 6: Comparison between VClim and the 20th century RCM simulations for mean daily rainfall (top row) and the 5-year event magnitude (bottom row). The left and central columns show the percentage difference between the two RCM simulations and the VClim data set. The right column shows the percentage difference between the RCM reanalyses and RCM control runs.

The ERA-40 data set was created by assimilating numerous observations into a dynamical model in a way that maintained a physically consistent solution. As such it represents the "best guess" at the true state of the atmosphere and it is expected

that the RCM reanalysis should not have contained any significant circulation biases. However, the GCM, used to drive the RCM control, did contain circulation biases, including an increase in the strength of the westerly circulation. This resulted in the east-west gradient in the mean precipitation over the South Island decreasing by between 10 and 20% from the Reanalyses to the Control (Figure 6; top right). However, the error in the Control compared to VClim was about 50% in the east and 100% in the west (Figure 6; top left). Hence the circulation biases in the GCM only accounted for a small fraction of the mean rainfall bias in the control simulation. The remaining bias is hypothesised to be due to the topography of the RCM, the parameterization of the rainfall processes used by the model or biases in the VClim rainfall surface.

Unlike the changes in mean rainfall, the biases in the simulation of the 5-year event magnitude were substantially reduced in the reanalysis simulation, mainly over the North Island (Figure 6; bottom row). The reasons for this may be partially related to biases in the mean circulation of the GCM, however other factors may also have played a part. For example, extreme precipitation is dependant on humidity and it is possible that the GCM was biased in this field with respect to the ERA-40 data set. Additionally, the ERA-40 simulation contained a representation of the actual storms that passed over New Zealand, while the GCM may not have had the correct type, or number of storms. This last point, while not necessarily affecting the mean precipitation, may have had a significant impact on outlier events and therefore extreme precipitation.

4) SITE SPECIFIC COMPARISON

In order to further investigate the cause of the differences in extreme rainfall between the RCM control and gridded observations, rainfall records from the climate stations shown in Figure 1 were examined. The 5-year event for each station and for the grid point nearest to the station in the gridded observations, the RCM control and the RCM reanalyses run is shown in Figure 7. For all stations except Outram, the event magnitude from the VClim data set was less than that from the actual station. This was most obvious for the wet sites shown in Figure 7b. For both dry and wet sites,

the range of event magnitudes from the RCM control was much more consistent with the station data than with the VClim data.

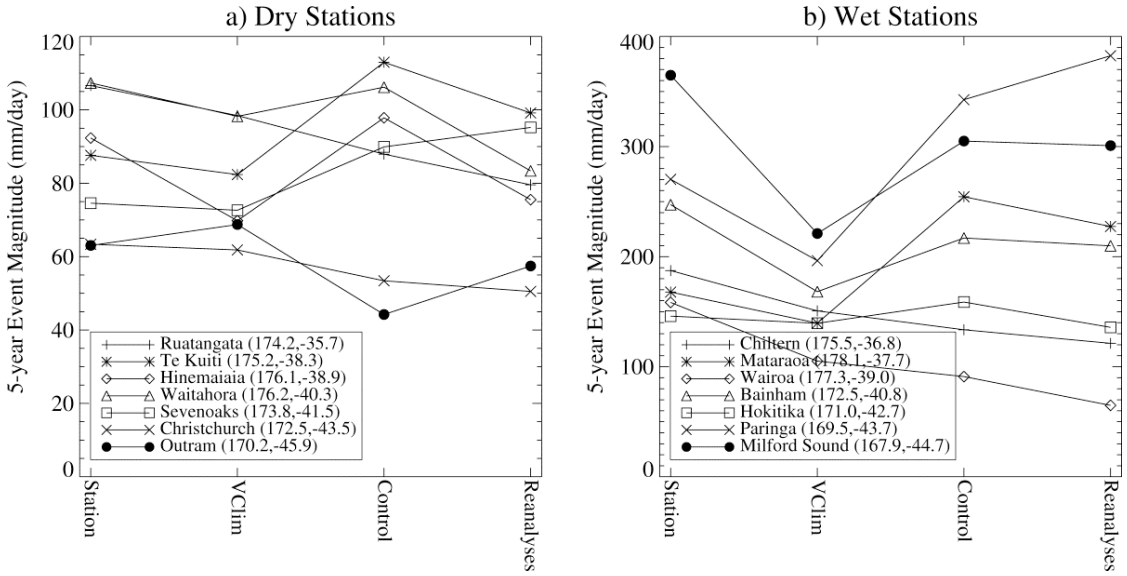

Figure 7: Comparison of 5-year event magnitude calculated from the climate station time series (Station), the gridded observations (VClim), the RCM control run and the RCM driven by ERA-40 reanalyses. Relatively dry stations (a) and wet stations (b) are arbitrarily separated to allow for different y-axis scales.

These results again indicate that the gridded observations may underestimate extreme precipitation events, particularly in mountainous areas (for example Hinemaiaia) and very wet regions. This would account for some of the discrepancy between the RCM and VClim observed in Figure 5.

b. Simulated Changes in Precipitation Extremes

Precipitation extremes for the future climate (2072—2100) as simulated by the regional climate model were compared with those derived from the present climate (control simulation) and the absolute and percentage change in the 5-year rainfall event magnitude distributions are presented in Figure 8. All of the future simulations had larger event magnitudes than the control over most of the country. Only the southwest tip of the South Island had a consistent decrease in event magnitude in all three simulations. The strongest percentage changes were in the north of the North

Island and the east coast of the South Island. The largest absolute increases in event magnitude were on the west of the Southern Alps and in the Bay of Plenty.

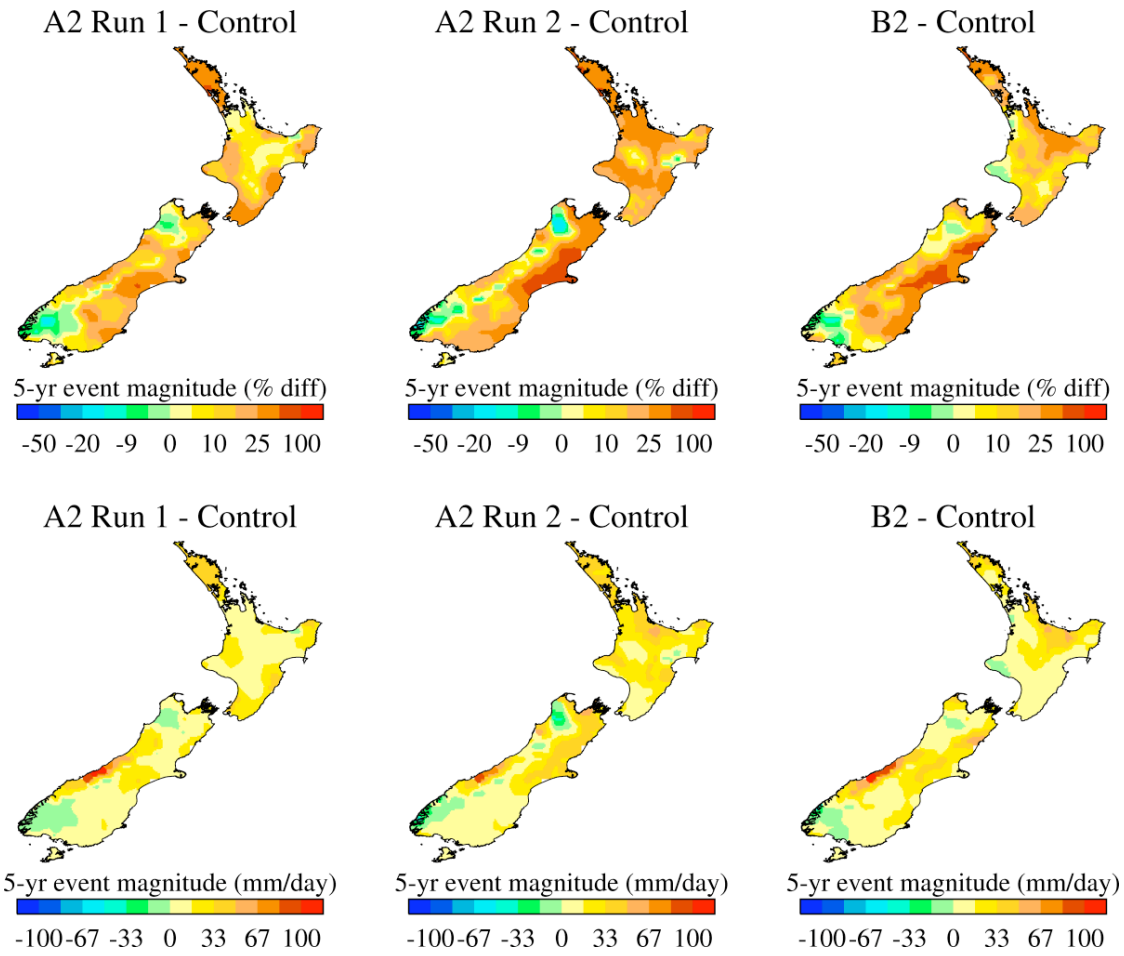

Figure 8: Percentage (top) and absolute (bottom) difference plots showing the change in 5-year rainfall event magnitude between the RCM control and the 3 future RCM runs.

It is interesting to note that in terms of the statistics presented in Figure 8, the second A2 simulation had more in common with the B2 simulation than with the first A2 simulation. This suggests that the inherent variability in extreme precipitation events was more significant than any change the difference in mean temperature between these two scenarios might have produced, at least for short return-interval extremes. To investigate this further, Figure 9 shows the area-averaged 5-year rainfall event magnitude for each of the six climate regions introduced in Figure 1.

The gridded observations had a lower (or very similar) event magnitude than both the 20th century RCM runs in all regions except the south east of the North Island. As was shown in Figure 7, this is likely to be a result of the interpolation scheme smoothing out many observed extreme rainfall events.

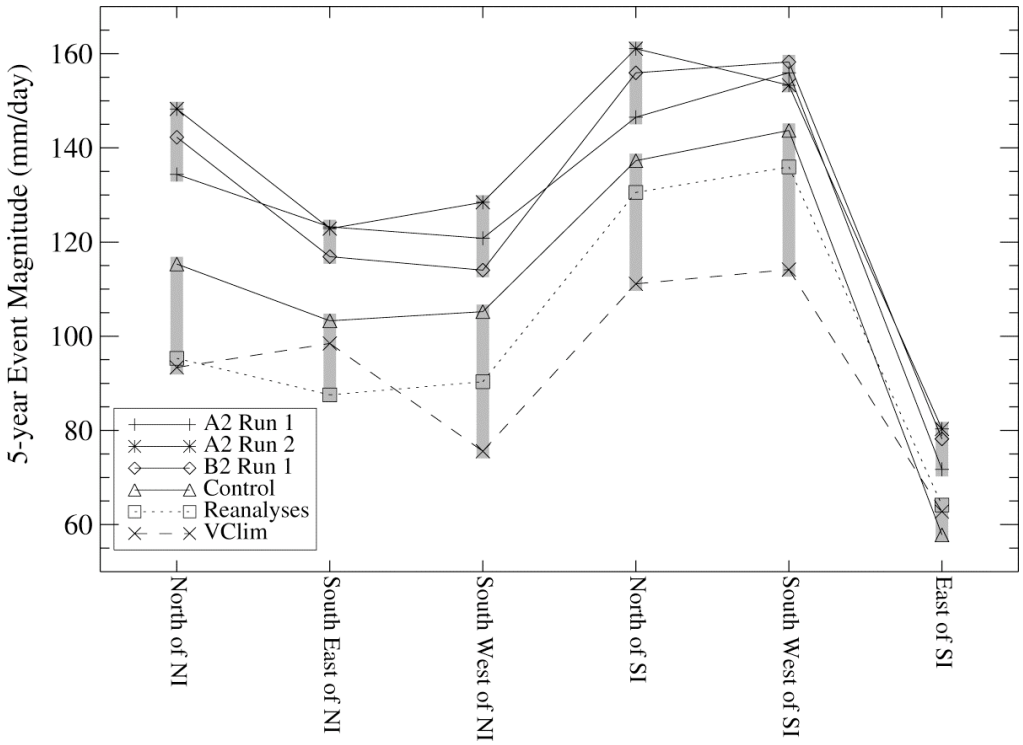

Figure 9: Variation in the extreme precipitation event magnitude over six different climatic zones within New Zealand. Data are shown from 4 free running RCM simulations (solid lines), the RCM constrained by ERA40 reanalyses (dotted line) and the VClim regridded observations (dashed line).

Figure 9 also shows that the future simulations had larger event magnitudes than the 20th century simulations for all six climate regions. However, no one RCM simulation had the strongest events across all regions, in fact there was considerable overlap and variability between the different model runs. In addition, for all three scenarios, the parent global model was identical. It is likely that additional regional variability would be introduced if it was possible to use a variety of driving global models. Altogether, this suggests that this limited set of three thirty year simulations

driven by one global model was insufficient to accurately quantify any regional differences in changes in extreme precipitation due to climate change.

c. Factors Limiting Changes in Precipitation Extremes

According to the Clausius-Clapeyron constraint, the maximum amount of available moisture in the atmosphere increases by about 6.5% per degree of warming (Boer, 1993; Held and Soden, 2000). It has been suggested that extreme precipitation events are those that occur when all available moisture has been precipitated out, and therefore that the magnitude of extreme precipitation events will also increase by about 6.5%/K (Allen and Ingram, 2002; Pall *et al.*, 2007; Trenberth, 1999). However, recent studies have shown that extreme precipitation scales not only with moisture content, but also with the vertical profile of vertical velocity and the moist adiabatic temperature lapse rate (O'Gorman and Schneider, 2009; Sugiyama *et al.*, 2010). Results from WCRP global climate models suggest that precipitation extremes increase more slowly than moisture content in the extra-tropics (O'Gorman and Schneider, 2009), whereas in the tropics changes in precipitation extremes often exceed those in water vapour content (Sugiyama *et al.*, 2010). Therefore, using the value of 6.5%/K to estimate the changes in precipitation extremes is likely to give incorrect predictions, particularly when attempting to estimate changes on a regional scale.

In theory, it should be possible to estimate the maximum expected precipitation change per degree of warming using extreme value theory. However, the tendency of the GPD to use a positive shape parameter on these relatively short time series, as discussed above, means that the change per degree of warming increases exponentially with increasing return period. The model data does not support this result, and it is reasonable to postulate that there are physical processes in the atmosphere that are likely to restrict extreme precipitation increases to some limit, albeit different from 6.5%/K.

The question then remains as whether it is possible to predict the likely change in high return period events from such short data series. Figure 10 is a logarithmic percentile plot of the percentage change in rainfall amount per degree of regional warming. Percentiles were calculated for control and future data sets

separately and the percentage change at each percentile (normalised by the regional temperature change) is presented. These calculations included all data for the domain of the Regional Climate Model, both land and sea points, which increased the number of data points available to describe the tails of the distribution, but meant that the data was no longer independent. Extreme precipitation events are mainly to be found in certain areas in the domain (for example the west coast of the South Island) therefore the conclusions drawn below are not representative of the entire domain, but are useful in describing changes in regions of heavy precipitation. In addition, because the data in Figure 10 is not from a single location, the percentiles can not be meaningfully converted to average return intervals as was done for Figure 4.

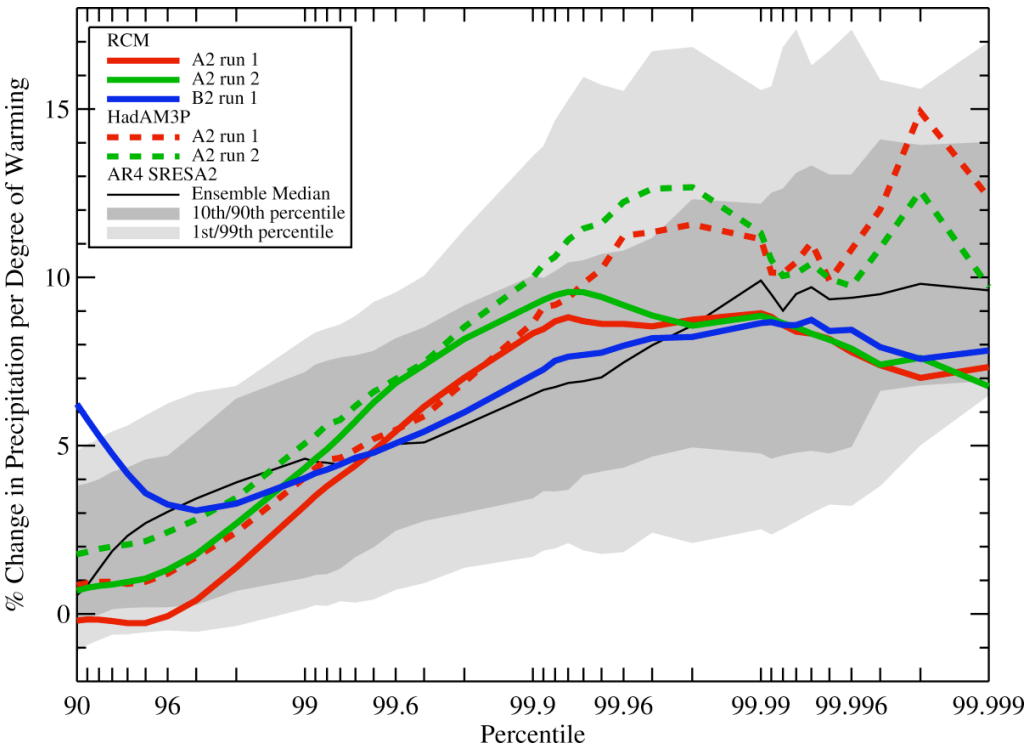

Figure 10: The percentage change in precipitation (per degree of regional warming) under the A2 emission scenario for the RCM, its parent GCM (HadAM3P) and an ensemble of 16 CMIP3 climate models.

As was inferred for Milford Sound alone (Figure 4), the percentage change in precipitation over the RCM domain became relatively constant above the 99.9

percentile. Also shown in Figure 10 is the percentage change in precipitation per degree of warming (over the RCM domain) for the RCM's driving model (HadAM3P). These global runs showed a similar pattern, although the percentage change was nearly always greater than the RCM. For the global model runs, the percentage change became relatively constant above the 99.95 percentile. This was slightly higher than for the RCM and may have resulted from the GCM's lower resolution and therefore lower absolute values of extreme precipitation events. For both the RCM and its driving model, the increase in extreme precipitation was somewhat greater than the CC constraint of 6.5%.

Also included in Figure 10 is the change in precipitation over the domain of the regional climate model for an ensemble of 16 WCRP CMIP3 global climate models for which simulations under the A2 emissions scenario were available. These models were used in an attempt to quantify the spread that might be expected from model uncertainties, compared to using only one model. The median of the ensemble reached an increase of 10%/K, which was slightly lower than for the HadAM3P global runs, however as the shading indicates, the spread of the CMIP3 models was quite wide and encompassed the individual model runs. For example, at the 99.99 percentile 80 percent of the ensemble showed a change of between 5 and 12 %/K.

Given that the RCM's dynamical downscaling of the GCM output reduced the expected change in precipitation extremes, it might be expected that when downscaling the CMIP3 models to a regional scale, the precipitation changes would also be reduced.

4. Conclusion

Simulation of precipitation extremes by a regional climate model has been validated using a daily observed rainfall surface (VClim) and site-specific climate station observations. While comparisons with climate station observations were very good, significant biases existed between the RCM and VClim, partly due to the smoothing introduced in the creation of the observed rainfall surface.

Twenty-first century regional simulations under the A2 and B2 emissions scenarios showed that precipitation extremes are likely to increase over most, if not all, of New Zealand in a future, warmer, climate. However, it was not possible to identify regions of New Zealand in which increases in precipitation extremes were likely to be higher or lower than average. Three thirty year simulations each showed significant variation in the regions of higher than average extremes and also represented only one driving model. Use of the Generalised Pareto Distribution for fitting to the tails of modelled rainfall distributions was found to be fraught with difficulty. The tendency for fitting negative shape parameters resulted in an ever increasing percentage change in rainfall extremes for higher return periods. When the threshold was set high enough to ensure a negative shape parameter, the fits became very unstable. This suggested that a higher order polynomial may be necessary for studies which do not wish to make use of an *a-priori* assumption about the shape of the distribution. As such the fitted GPD curves were not used to extrapolate beyond the 5 year return period.

By examining the full RCM domain covering New Zealand and the surrounding ocean, an estimate of the maximum expected change in extreme precipitation as a function of regional warming was found to be between 7 and 9 %/K. Results from an ensemble of global climate models suggested the likely range to be 5 to 12 %/K. While this may give reasonable guidance for wet areas of the country it is likely that changes in drier areas may be more complicated.

The current standard guidance available for councils and engineers in New Zealand who are planning for extreme rainfall changes under future climates is available in Mullan *et al.* (2007). Table 5.2 of this report suggested a maximum increase of 8% per degree of warming for all return periods and rainfall durations, a number derived principally from the Clausius-Clapeyron constraint. The recent understanding as to why climate models do not generally obey this theoretical constraint, combined with the results of this analysis, suggest that planners should be considering a wider range of increases.

Acknowledgements

We acknowledge the modelling groups, the Program for Climate Model Diagnosis and Intercomparison (PCMDI) and the WCRP's Working Group on Coupled Modelling (WGCM) for their roles in making available the WCRP CMIP3 multi-model data set. Support of this data set is provided by the Office of Science, U.S. Department of Energy.

References

Allen, M. R. and W. J. Ingram, 2002: Constraints on future changes in climate and the hydrologic cycle. *Nature*, **419,** 224-227+229-232.

Boer, G. J., 1993: Climate change and the regulation of the surface moisture and energy budgets. *Climate Dynamics*, **8,** 225-239.

Brabson, B. B. and J. P. Palutikof, 2000: Tests of the generalized Pareto distribution for predicting extreme wind speeds. *Journal of Applied Meteorology*, **39,** 1627-1640.

Coles, S. G., 1994: A temporal study of extreme rainfall. *Statistics for the Environment, Vol. 2, Water Related Issues*, **2,** 61-78.

——, 2001: *An introduction to statistical modeling of extreme values*. *Springer Series in Statistics*, Springer-Verlag, 208 pp.

Frei, C., R. Scholl, S. Fukutome, J. Schmidli, and P. L. Vidale, 2006: Future change of precipitation extremes in Europe: Intercomparison of scenarios from regional climate models. *Journal of Geophysical Research D: Atmospheres*, **111**.

Griffiths, G. M., 2007: Changes in New Zealand daily rainfall extremes 1930-2004. *Weather and Climate*, **27,** 3-44.

Held, I. M. and B. J. Soden, 2000: Water vapor feedback and global warming. *Annual Review of Energy and the Environment*, **25,** 441-475.

Hosking, J. R. M., 1990: L-moments: Analysis and estimation of distributions using linear combinations of order statistics. *J. R. Stat. Soc., Ser. B*, **52,** 105-124.

Hosking, J. R. M. and J. R. Wallis, 1987: Parameter and quantile estimation for the generalized pareto distribution. *Technometrics*, **29,** 339-349.

Jones, R. G., M. Noguer, D. C. Hassell, D. Hudson, S. S. Wilson, J. G.J., and J. F. B. Mitchell, 2004: Generating high resolution climate change scenarios using PRECIS, *Met Office Hadley Centre*, Exeter, UK, 40 pp.

Jones, R. G, J. M. Murphy, D. C. Hassell, M. J. Woodage, 2005: A high resolution atmospheric GCM for the generation of regional climate scenarios. *Hadley Centre Technical Note 63*, Met Office, Exeter, UK.

Li, Y., W. Cai, and E. P. Campbell, 2005: Statistical modeling of extreme rainfall in southwest Western Australia. *Journal of Climate*, **18,** 852-863.

Madsen, H., D. Rosbjerg, and P. Harremoes, 1994: PDS-modelling and regional Bayesian estimation of extreme rainfalls. *Nordic Hydrology*, **25,** 279-300.

Madsen, H., P. F. Rasmussen, and D. Rosbjerg, 1997: Comparison of annual maximum series and partial duration series methods for modeling extreme hydrologic events 1. At-site modeling. *Water Resources Research*, **33,** 747-757.

May, W., 2007: The simulation of the variability and extremes of daily precipitation over Europe by the HIRHAM regional climate model. *Global and Planetary Change*, **57,** 59-82.

Meehl, G. A., C. Covey, T. Delworth, M. Latif, B. McAvaney, J. F. B. Mitchell, R. J. Stouffer, and K. E. Taylor, 2007: The WCRP CMIP3 multi-model dataset: A new era in climate change research, *Bulletin of the American Meteorological Society*, **88**, 1383-1394.

Mullan, A. B., 1998: Southern Hemisphere sea surface temperatures and their contemporary and lag association with New Zealand temperature and precipitation. *International Journal of Climatology* **18**, 817-840.

Mullan, B., D. Wratt, S. Dean, M. Hollis, S. Allan, T. Williams, and G. Kenny, 2007: Climate Change Effects and Impacts Assessment: A guidance manual for local government in New Zealand updated 2007. WLG2007/62. Available from www.mfe.govt.nz.

Nakicenovic, N., J. Alcamo, G. Davis, B. de Vries, J. Fenhann, S. Gaffin, K. Gregory, A. Gruebler, T. Y. Jung, T. Kram, E. L. La Rovere, L. Michaelis, S. Mori, T. Morita, W. Pepper, H. Pitcher, L. Price, K. Riahi, A. Roehrl, H.-H. Rogner, A. Sankovski, M. Schlesinger, P. Shukla, S. Smith, R. Swart, S. van Rooijen, N. Victor, and Z. Dadi, 2000: Special report on emissions scenarios: A special report of Working group III of the Intergovernmental Panel on Climate Change. *Cambridge University Press, Cambridge, UK*, 599 pp.

O'Gorman, P. A. and T. Schneider, 2009: The physical basis for increases in precipitation extremes in simulations of 21st-century climate change. *Proceedings of the National Academy of Sciences of the United States of America*, **106,** 14773-14777.

Pall, P., M. R. Allen, and D. A. Stone, 2007: Testing the Clausius-Clapeyron constraint on changes in extreme precipitation under CO2 warming. *Climate Dynamics*, **28,** 351-363.

Pandey, M. D., P. H. A. J. M. Van Gelder, and J. K. Vrijling, 2001: The estimation of extreme quantiles of wind velocity using L-moments in the peaks-over-threshold approach. *Structural Safety*, **23,** 179-192.

Pickands, J., 1975: Statistical inference using extreme order statistics. *Annals of Statistics*, **3,** 119-131.

Rosbjerg, D., H. Madsen, and P. F. Rasmussen, 1992: Prediction in partial duration series with generalised Pareto- distributed exceedances. *Water Resources Research*, **28,** 3001-3010.

Rowell, D. P., 2005: A scenario of European climate change for the late twenty-first century: seasonal means and interannual variability. *Climate Dynamics*, **25**, 837–849, DOI 10.1007/s00382-005-0068-6.

Sugiyama, M., H. Shiogama, and S. Emori, 2010: Precipitation extreme changes exceeding moisture content increases in MIROC and IPCC climate models. *Proceedings of the National Academy of Sciences of the United States of America*, **107,** 571-575.

Tait, A., R. Henderson, R. Turner, and X. Zheng, 2006: Thin plate smoothing spline interpolation of daily rainfall for New Zealand using a climatological rainfall surface. *International Journal of Climatology*, **26,** 2097-2115.

Trenberth, K. E., 1999: Conceptual framework for changes of extremes of the hydrological cycle with climate change. *Climatic Change*, **42,** 327-339.

Yiou, P., K. Goubanova, Z. X. Li, and M. Nogaj, 2008: Weather regime dependence of extreme value statistics for summer temperature and precipitation. *Nonlinear Processes in Geophysics*, **15,** 365-378.

Submitted to Weather and Climate March 2010, Revised June 2010